

---

# Co-extrusion of biocompatible polymers for scaffolds with co-continuous morphology

---

Newell R. Washburn, Carl G. Simon, Jr., Alessandro Tona, Hoda M. Elgendy, Alamgir Karim, Eric J. Amis  
Polymers Division, National Institute of Standards and Technology, 100 Bureau Drive, Stop 8542,  
Gaithersburg, Maryland 20899

Received 12 December 2001; revised 10 August 2001; accepted 16 August 2001

**Abstract:** A methodology for the preparation of porous scaffolds for tissue engineering using co-extrusion is presented. Poly( $\epsilon$ -caprolactone) is blended with poly(ethylene oxide) in a twin-screw extruder to form a two-phase material with micron-sized domains. Selective dissolution of the poly(ethylene oxide) with water results in a porous material. A range of blend volume fractions results in co-continuous networks of polymer and void spaces. Annealing studies demonstrate that the characteristic pore size may be increased to larger than 100  $\mu\text{m}$ . The mechanical properties of the scaffolds are characterized by a compressive modulus on the order of 1 MPa at low strains but displaying a marked strain-dependence. The results of osteoblast seeding suggest

it is possible to use co-extrusion to prepare polymer scaffolds without the introduction of toxic contaminants. Polymer co-extrusion is amenable to both laboratory- and industrial-scale production of scaffolds for tissue engineering and only requires rheological characterization of the blend components. This method leads to scaffolds that have continuous void space and controlled characteristic length scales without the use of potentially toxic organic solvents. © 2002 John Wiley & Sons, Inc. \* J Biomed Mater Res 60: 20–29, 2002

**Key words:** polymers scaffolds; polymer processing; tissue engineering; bone replacement materials; biocompatibility

---

## INTRODUCTION

Increased understanding of how the body interacts with metals, ceramics, and polymers in medical implants is leading to the development of new biocompatible materials.<sup>1</sup> One area of great current interest is the field of tissue engineering in which a material is used as a scaffold to grow new tissue, either *in vitro* or *in vivo*.<sup>2</sup> The goal in tissue engineering is to provide an environment in which cells may proliferate in a manner that leads to tissue development. Certain cell types have been shown to grow very effectively in porous

media including bone,<sup>3</sup> cartilage,<sup>4</sup> and skin<sup>5</sup> cells and much work in this area has been performed in the last 20 years. The development of new methods for creating such structured materials is a central concern. Polymeric materials satisfy many of the criteria necessary for generating tissue replacements; these include a similar hardness as surrounding tissue,<sup>6</sup> light weight, biocompatibility,<sup>7</sup> and biodegradability.<sup>8</sup> Furthermore, polymers may be processed using a wide range of methods that lead to control over the shape of the final product.

According to ISO 31-8, the term “molecular weight” has been replaced by “relative molecular mass,”  $M_r$ . The conventional notation, rather than the ISO notation, has been used for this article.

Certain equipment and instruments or materials are identified in this article to adequately specify the experimental details. Such identification neither implies recommendation by the National Institute of Standards and Technology, nor that the materials are necessarily the best available for the purpose.

Correspondence to: N. R. Washburn; e-mail: newell.washburn@nist.gov

The materials used as scaffolds for cell growth ideally have porous structures with characteristic length scales on the order of, or larger than, cellular dimensions. Many techniques have been developed for creating such open structures; one of the most widely used methods involves solvent casting a mixture of polymer and salt crystallites of well-controlled size.<sup>9</sup> After the solvent is removed, the salt is leached out with water resulting in voids the size and shape of the crystallites. This procedure has the advantage that it is relatively easy to prepare porous materials on the benchtop and the size of the voids may be varied continuously. Pore sizes up to 700  $\mu\text{m}$  have been produced using this technique.<sup>10</sup> Extrusion has been used in processing polymers blended with salt particles in simple extruders that rely solely on extensional flow at

elevated temperatures to achieve modest control over pore diameter at constant particle size.<sup>11</sup> Methods such as solid-liquid<sup>12,13</sup> or liquid-liquid<sup>14,15</sup> phase separation, microparticle aggregation,<sup>16</sup> and three-dimensional printing,<sup>17,18</sup> have also been investigated to generate porous polymeric materials for medical applications. Many of these techniques involve the use of organic solvents in the scaffold production, require detailed knowledge of polymer-solvent phase diagrams, or may not be amenable to molding the implant for clinical applications. We demonstrate here that extrusion of immiscible polymers, in which one of the polymers is water soluble, followed by selective dissolution, can be used to make porous materials with controlled pore sizes and connectivity without the difficulties associated with these other methods. To our knowledge, this technique has not been applied previously to produce polymeric scaffolds for tissue engineering. Furthermore, with careful cleaning of the apparatus, it is possible to blend polymers without the introduction of toxic contaminants.

Co-extrusion is an established method for blending polymers.<sup>19,20</sup> The extruder barrel is heated to the processing temperature (above the glass transition temperatures  $T_g$  and melting temperatures  $T_m$  of all components) and polymers are added and mechanically mixed. Factors that control the morphology of the extruded material are the volume fraction and viscosity of each polymer, the interfacial tension between the phases, and the mixing conditions (temperature, shear rate, etc., of which the viscosities and, to a lesser degree, the interfacial tension are a function).

In this work, a research-scale twin-screw extruder was used to blend poly( $\epsilon$ -caprolactone) (PCL), a biodegradable polyester, and poly(ethylene oxide) (PEO). After further processing, the PEO is dissolved, resulting in a porous material. Blending PCL with PEO has two advantages, the first is that PEO is water-soluble and potentially toxic organic solvents are not necessary to dissolve this phase. The second is that PEO is itself biocompatible and any residual polymer should not induce an inflammatory response.<sup>21</sup> A schematic of the extruder barrel is shown in Figure 1. Two screws rotate in tandem, driving material from the top of the barrel to the bottom then through a recirculation channel. Higher rotation rates lead to a more finely mixed blend. The blended polymers are recovered by opening the exit port at the bottom of the barrel and recovering the blend in the form of a tube, roughly 3 mm in diameter.

To allow the cells to permeate the scaffold, a continuous network of pores is necessary. In the extrusion method described here, this requires the generation of a polymer blend having a co-continuous structure. At a volume fraction of blend component A  $>0.16$ , the percolation threshold is crossed<sup>22</sup> and the resulting morphology, in principle, becomes co-continuous.

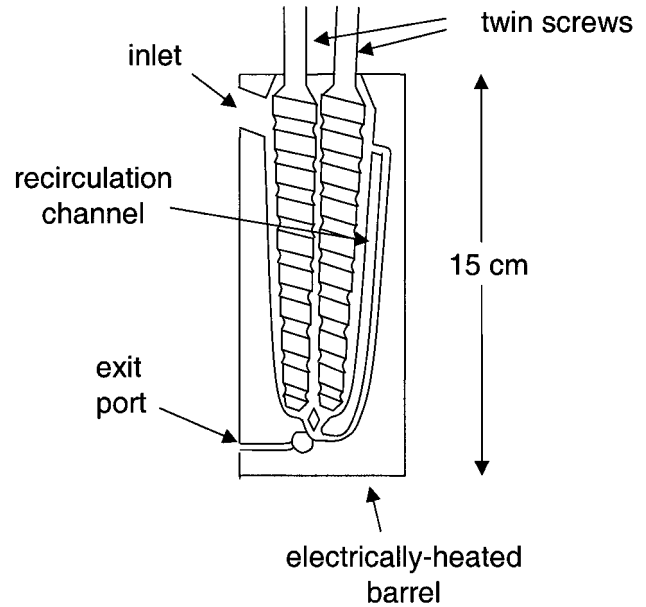


**Figure 1.** Picture of the extruder barrel used to blend the polymers. The twin screws rotate in tandem, driving material from the top of the barrel to the bottom then returning through the recirculation channel. The components are introduced through the inlet and the blend is recovered by opening the exit port at the bottom of the barrel.

There are several empirical relations that describe the point of phase inversion, the composition at which the blend is co-continuous and the mean curvature of the blend interface is zero. Paul and Barlow<sup>23</sup> and Jordhamo et al.<sup>24</sup> proposed the following relation:

$$\frac{\phi_A}{\phi_B} = \frac{\eta_A(\dot{\gamma})}{\eta_B(\dot{\gamma})} \quad (1)$$

which agrees with experimental data reasonably well. This equation may be qualitatively understood as follows. Consider a two-component blend composed of high- and low-viscosity materials in a homogeneous stress field. The component with the higher viscosity will tend to distort less and form droplets whereas the component with the lower viscosity will distort more. Thus, even in a blend with equal volume fractions of the two components, the lower-viscosity component may form a continuous matrix with isolated domains of the higher-viscosity component.<sup>25,26</sup>

Annealing above the  $T_g$  and  $T_m$  of all components in the absence of an applied stress field allows the domains to coarsen. In the initial stages of the coarsening of a co-continuous blend, the structure is maintained but the characteristic length scale increases linearly with time and the rate of increase is found to depend on the zero-shear viscosities of the blend components.<sup>27</sup> For the polymers used in this study, which have relatively low melting points and high viscosities, experimental determination of the appropriate

combination of annealing temperature and time led to a good deal of control over the resultant morphology.

## EXPERIMENTAL

### Materials

PCL ( $M_n = 80,000$  g/mol,  $\rho = 1.15$  g/cm<sup>3</sup>; Aldrich), poly(D,L-lactic acid) ( $M_n = 120,000$  g/mol; Alkermes), and PEO ( $M_n = 100,000$  g/mol, mass fraction 5% CaCO<sub>3</sub> and amorphous SiO<sub>2</sub>,  $\rho = 1.2$  g/cm<sup>3</sup>; Polysciences) were used as received. All compositions listed are either on the basis of volume fraction or volume percent. Methanol (Fisher) was used as received. Deionized water with a resistivity of 15 M $\Omega$  · cm was used to dissolve the PEO. The substrate used for polymer film studies was a polished silicon wafer (Wafer World, Inc.) that was exposed to UV light for 5 min to create a hydrophilic surface. After UV treatment, the wafer was immersed in 2% solution (by mass) of chlorodimethyloctylsilane (Aldrich) in toluene (Fisher) for 30 min, gently rinsed in toluene, and placed under vacuum at 150°C for 2 h. This creates a hydrophobic surface that PCL will wet.

### Dynamical mechanical spectrometry

Measurements were performed on a Rheometrics Stress Rheometer using a parallel plate configuration with a sample thickness of 0.5 mm. The rheometer gap was zeroed at 100°C but samples were loaded at 150°C and the plates were lowered until the sample filled the gap. Samples were kept under a flow of N<sub>2</sub> gas to minimize degradation. The temperature was lowered to 100°C and the sample was annealed for 20 min. The gap was then decreased to 0.5 mm and the excess polymer shaved off the sides of the sample holder. After annealing for 30 min, stress-strain curves were obtained to determine the linear response regime. For both polymers, a stress-amplitude of 100 Pa at 1 rad/s was applied for the frequency-dependent measurements. This led to strains below 5%, well within the linear regime.

### Extrusion

Polymers were blended using a twin-screw minicomponenter (Daca Instruments, Goleta, CA). The instrument was cleaned by the following procedure. First the barrel was sealed and filled with toluene for 20 min. After draining the toluene, chloroform was loaded and drained after 20 min. Finally, the extruder was heated to 100°C and five batches of the PCL/PEO blend (total mass 3.5 g) were mixed at 100°C for 10 min. The blends were removed by opening the exit port and allowing the polymers to be forced out of the barrel. Running these multiple batches removes residual contaminants in the extruder barrel that are soluble in the polymers. Note that this procedure is done only to

remove potentially toxic contaminants from previous blending of non-biocompatible polymers. The cleanliness of the extruder can then be maintained almost indefinitely just by scraping out residual polymers between runs so long as only biocompatible materials are compounded. After cleaning, the blend components were added to the extruder simultaneously using a funnel tool and mixed at 50 rpm for 10 min at temperature. The blend was recovered by opening the exit port and allowing the material to flow out of the extruder in the form of a tube, approximately 3 mm in diameter. Blends are referred to by the volume fraction of PCL, e.g., 30% PCL.

### Annealing studies

The extruded tubes were cut with a razor into cylinders 4-mm long and annealed in a vacuum oven at 80°C, above the melting temperatures of both PEO and PCL. The samples are removed from the oven and pressed flat to a thickness of 1 mm. These were placed in water-filled test tubes and agitated on a rocking stage (New Brunswick Scientific) at 100 cycles/min. After 48 h, the samples were removed from the test tubes, rinsed with methanol, and placed in a vacuum oven at room temperature for 8 h. The samples were then weighed and the mass was found to be consistent with that expected for essentially complete dissolution of the PEO.

### Scanning electron microscopy

Scaffolds were rinsed with methanol, dried under vacuum, and sputter-coated with gold before imaging. Scanning electron micrographs were obtained with a Jeol JL-5300 operating at 5 kV and 50 mA.

### Compression testing

Compressive moduli of annealed scaffolds were measured using an Instron 5500R on disk-shaped samples with 0.5-cm height and 2-cm diameter. Although these dimensions do not conform to ASTM specifications, they were chosen to ensure that the sample microstructure was homogeneous after annealing and PEO dissolution. Compression was done at 0.5 mm/s. Data were obtained as load as a function of displacement, which was converted to stress as a function of strain by measuring the sample area and thickness. No attempts to correct for sample porosity were made.

### Polymer film preparation

Solutions of 5% PCL in toluene (by mass) were prepared and cast onto a silanized silicon wafer using a home-built flow-coater and annealed under vacuum at 80°C for 4 days to remove residual solvent.

### Contact angle measurement

Water contact angles were measured with a Krüss Contact Angle Measuring System G2. Drops of deionized water with volumes of approximately 5  $\mu\text{L}$  were placed on the film and the contact angle was measured using the tangent method.

### Cell culture

Established protocols for the culture and passage of MC3T3-E1 cells were followed.<sup>28</sup> Cells were obtained from Riken Cell Bank (Hirosaka, Japan) and cultured in flasks (75-cm<sup>2</sup> surface area) at 37°C in a fully humidified atmosphere at 5% CO<sub>2</sub> (volume fraction) in a modification of Eagle's minimum essential medium (Biowhittaker, Inc., Walkersville, MD) supplemented with 10% (volume fraction) fetal bovine serum (Gibco, Rockville, MD) and kanamycin sulfate (Sigma, St. Louis, MO). Media was changed twice weekly and cultures were passaged with 2.5 g/L trypsin (mass fraction 0.25%) and 1 mmol/L EDTA (Gibco) once per week. Cultures of 90% confluent MC3T3-E1 cells were trypsinized, washed, and suspended in fresh media. PCL scaffolds were conditioned for 7 days in serum-supplemented medium and placed separately into the wells of a 6-well plate. Fifty thousand cells diluted into 2 mL of media were added to wells containing the scaffolds or coverslips, incubated for 9 days, and then prepared for fluorescence microscopy or electron microscopy.

### Fluorescence microscopy

Cells were double-stained with calcein-AM and ethidium homodimer-1 (both from Molecular Probes) and observed with a fluorescence microscope. After incubation of the cells on the annealed scaffolds for 9 days, the media was removed and the scaffolds were washed two times in 2 mL of Tyrode's-HEPES buffer (140 mmol/L NaCl, 0.34 mmol/L Na<sub>2</sub>HPO<sub>4</sub>, 2.9 mmol/L KCl, 10 mmol/L HEPES, 12 mmol/L NaHCO<sub>3</sub>, 5 mmol/L glucose, pH 7.4). Cells were stained for 1 h with 2 mL of Tyrode's-HEPES buffer containing 2  $\mu\text{mol/L}$  calcein-AM and 2  $\mu\text{mol/L}$  ethidium homodimer-1 and viewed by epifluorescence microscopy (Olympus BH-2, Melville, NY). Calcein-AM is a nonfluorescent, cell-permeant fluorescein derivative, which is converted by cellular enzymes into cell-impermeant and highly fluorescent calcein. Calcein accumulates inside live cells having intact membranes causing them to fluoresce green. Ethidium-homodimer-1 enters dead cells with damaged membranes and undergoes a 40-fold enhancement of fluorescence upon binding their DNA, causing dead cells to fluoresce red. Double-staining cells anchored on the scaffolds allows simultaneous examination of both live and dead cells on the scaffolds. Cells grown on coverslips served as a control.

### Preparation of cell-seeded scaffolds for scanning electron microscopy

Cells were seeded on annealed scaffolds and cultured for 9 days. Following the procedure of Gear,<sup>29</sup> the medium was

replaced by 154 mmol/L saline solution then fixed with a volume fraction 1% glutaraldehyde/saline solution for 1 h. This was followed by rinsing twice with saline for 10 min, then rinsing with a series of water/ethanol solutions with increasing ethanol mass fractions of 0%, 25%, 50%, 70%, 95%, and 100% for 10 min each. In the final drying step, samples were rinsed with hexamethyldisilazane (Aldrich) and allowed to air-dry for 1 h.<sup>30</sup>

## RESULTS AND DISCUSSION

### Rheology

A log-log plot of the real and imaginary parts of the viscosity as a function of frequency for PCL at 100°C is shown in Figure 2(a). The real part of the viscosity represents viscous energy dissipation in the material under flow whereas the imaginary part represents stored elastic energy. The shapes of the curves are consistent with that commonly observed in polymer melts. For PCL sheared at high frequency (above 300 rad/s), the rate is too high for the polymer chains to effectively reorganize in response to the applied stress and more energy is stored elastically than dissipated ( $\eta'' > \eta'$ ). At 200 rad/s, the shear rate has reached a critical value in which the energy stored and energy dissipated per cycle is equal ( $\eta'' = \eta'$ ). As the shear rate is lowered, the imaginary part of the viscosity peaks at 30 rad/s then decreases approximately linearly with the decreasing shear rate, as expected for a linear viscoelastic medium. The real part of the viscosity approaches a constant value of 9100 Pa · s at low frequencies, the terminal viscosity.

The frequency-dependent rheological behavior of PEO displays the same features as PCL although with certain key differences in the actual values. The real and imaginary parts of the viscosity are equal at 80 rad/s but  $\eta''$  does not peak until 0.1 rad/s, more than two orders of magnitude lower than the frequency peak for PCL. Consequently, the terminal regime was not accessed in these experiments, although it appears that the terminal viscosity of the PEO used in these experiments is approximately 40000 Pa · s.

In these experiments, the shear rate around the extruder screws is estimated to be 10 rad/s, where  $\eta'$  and  $\eta''$  are nearly equal in PEO and  $\eta'$  exceeds  $\eta''$  by an order of magnitude in PCL. Significant viscoelastic effects are therefore expected, making quantitative predictions of the blend morphology difficult. To make comparisons between the two materials, the magnitude of the complex viscosity is used. This is known as the Cox-Merz rule<sup>31</sup> and although it is only an empirical relationship, it generally yields consistent predictions of blending behavior at higher shear rates. The

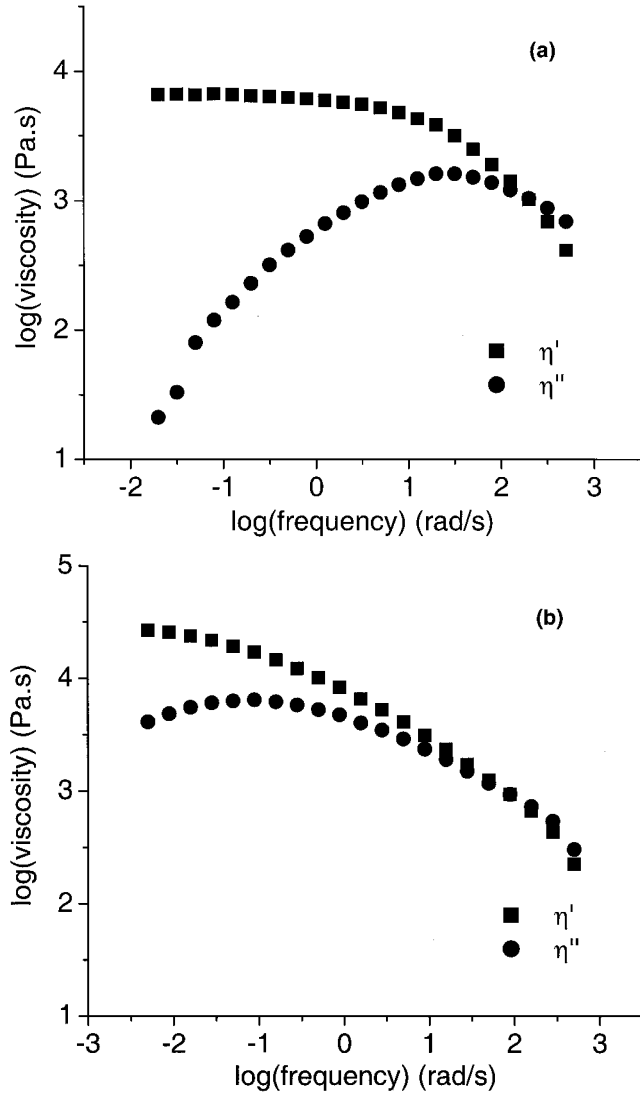


**Figure 2.** (a) Real and imaginary parts of the viscosity of PCL as a function of frequency at 100°C and a stress amplitude of 100 Pa. The real part of the viscosity is represented by squares and the imaginary part by circles. Blending was performed at approximately 10 rad/s. (b) Real and imaginary parts of the viscosity of PEO as a function of frequency at 100°C and a stress amplitude of 100 Pa. The estimated uncertainty in this measurement is 60 Pa · s.

values of  $|\eta(\omega = 10 \text{ rad/s})|$  obtained using this relation are 4700 Pa · s for PCL and 4200 Pa · s for PEO with a viscosity ratio of 1.1. Thus, on the basis of Equation (2), the blend morphology “phase diagram” is expected to be nearly symmetric, with the inversion point at  $\phi_{\text{PCL}} = 0.52$ . This estimate predicts co-continuous structures will be expected at compositions around 50% PCL although these structures are expected to be observed at a range of compositions. Factors such as interfacial tension also contribute to the range of compositions in which these structures are stable.<sup>32</sup>

### Unannealed blend structure

Blends of PCL and PEO with PCL volume fractions of 30 and 50% were prepared and both were found to yield co-continuous blends, which are of primary interest for tissue engineering applications. Compositions of 70% PCL were found to lead to blends with an unconnected minority phase and dissolution of the PEO resulted in closed, spherical pores. Compositions with 20% PCL result in scaffolds that crumble easily. Based on these experiments, the range of PCL volume fractions that result in co-continuous blends is approximately 25 to 60%. In this work, we compare two compositions, 30 and 50% PCL.

The 30% PCL sample, shown in Figure 3(a), has a striated appearance composed of PCL cords with a diameter of about 1  $\mu\text{m}$ . The PCL cords are mostly aligned with the axis of the extruded cylinder, along the direction of extensional flow as the blend exited the compounder. This sample retains its mechanical integrity even after the dissolution of the PEO, indicating that the PCL forms a continuous phase.

In Figure 3(b) is shown an electron micrograph of the unannealed 50% PCL sample. The surface is composed of similar 1- $\mu\text{m}$  diameter cords as observed in Figure 3(a) as well as broader PCL ribbons. The long axis of the extruded cylinder is from the top left to the bottom right in the image, and although there is evidence for some shear alignment along the flow-direction, it is not as extensive as in the 30% sample.

We attribute the shear alignment observed on the surface of the PCL phase to the extensional flow the material experiences as it exits the extruder. If we treat the exit port as a capillary rheometer, we may obtain estimates for the stresses necessary to generate the shear alignment observed in these blends.<sup>31</sup> Assuming a volumetric flow rate of 50  $\text{mm}^3/\text{s}$  and an exit port diameter of 1 mm, the Newtonian shear rate at the wall is calculated to be 64  $\text{s}^{-1}$ . For a 50:50 blend of PCL and PEO having a melt viscosity at 64  $\text{s}^{-1}$  on the order of 2000 Pa · s leads to a shear stress at the walls of approximately 0.1 MPa. This is a relatively high value, being on the order of the shear stresses at which surface instabilities such as sharkskin are observed in polymer processing.<sup>33</sup> Calculations of this type lead to estimates of the processing conditions necessary to produce anisotropic materials.

### Annealed blend structure

In Figures 4 and 5 are shown samples after annealing for 20 min at 80°C. At 30% PCL [Fig. 4(a)], the surface of the material forms an open, three-

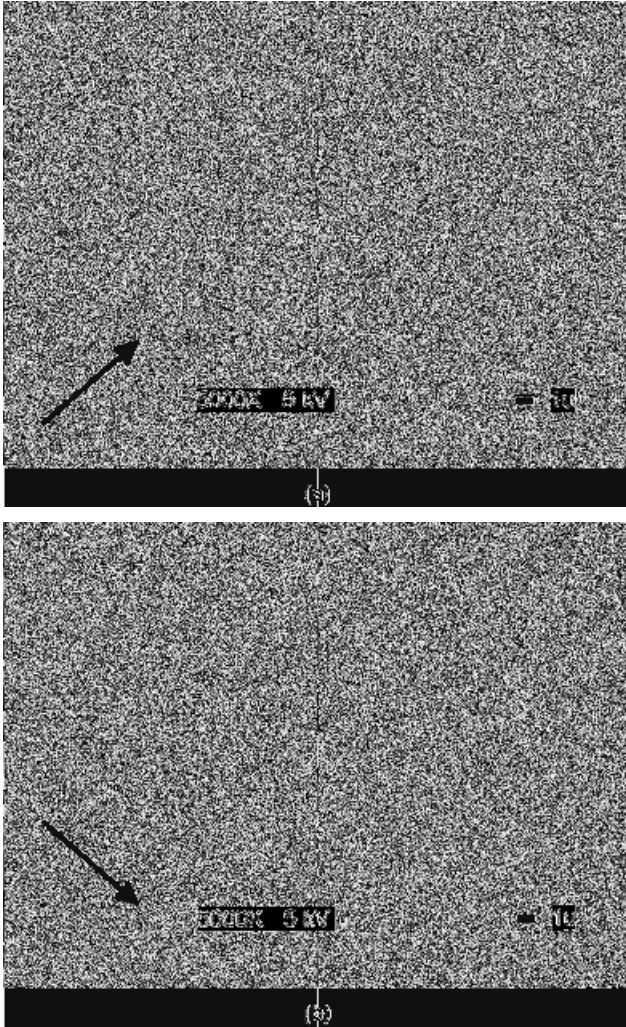


**Figure 3.** (a) Scanning electron micrograph of the surface of the 30% PCL sample after dissolution of PEO. Cords of PCL having an average diameter of 1  $\mu\text{m}$  are aligned along the main axis of the extruded cylinders. (b) Scanning electron micrograph of the 50% PCL sample after dissolution of PEO. The surface is composed of thinner cords and broader ribbons of PCL and less shear alignment is evident. The arrows in the lower left hand corner indicate the flow direction upon exiting the extruder and significant shear alignment is observed.

dimensional network with a characteristic void space length scale close to 100  $\mu\text{m}$ . The interior of the annealed 30% PCL sample is shown in Figure 4(b). The interior of the material was significantly perturbed by slicing the scaffold, even after cooling in liquid nitrogen. However, the interior is also characterized by a continuous void-network with pore diameters ranging from 20 to 150  $\mu\text{m}$ . It should be noted that the morphology of the void space in scaffolds produced using co-extrusion is qualitatively different than when dissolution of salt particles is used. The voids in these materials reflect the shape of the dissolved phase and co-extrusion results in curved surfaces whereas salt leaching results in approximately cubic voids.

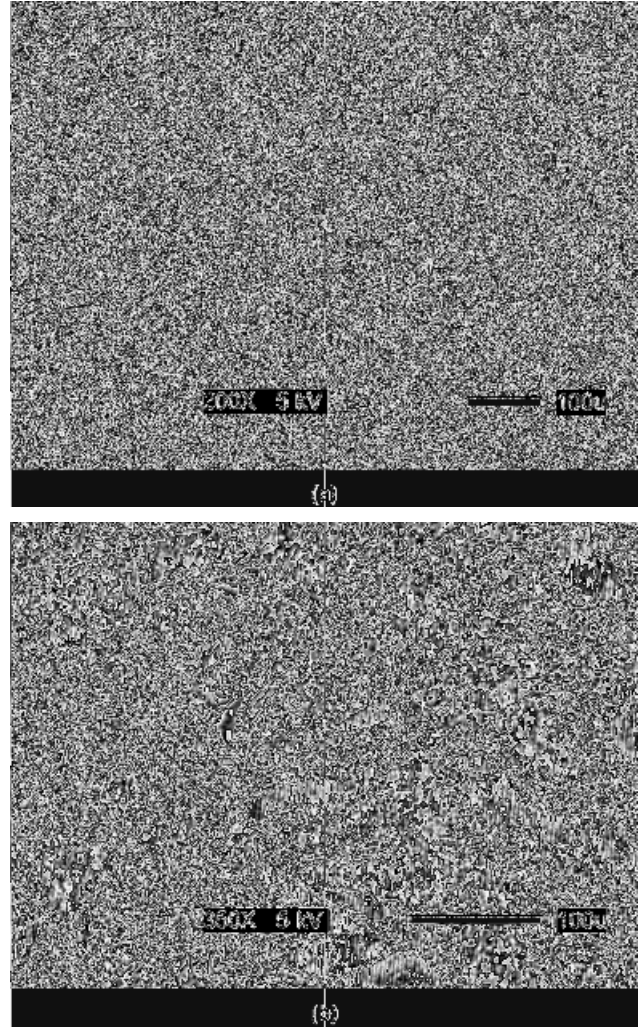


**Figure 4.** (a) Scanning electron micrograph of the surface of the 30% PCL sample after annealing for 20 min at 80°C and subsequent dissolution of PEO. The sample appears to have a continuous network of void space with a characteristic length scale of roughly 100  $\mu\text{m}$ . (b) Interior of the annealed 30% PCL sample that was exposed using a razor blade. The structure was obviously perturbed by cutting but it appears to be co-continuous with pores ranging from 20 to 150  $\mu\text{m}$ .

The surface of the sample with 50% PCL, shown in Figure 5(a), also has a three-dimensional network structure although the PCL domains are thicker and the material less open, as expected. The characteristic length scale of the pores is smaller for this sample, closer to 20  $\mu\text{m}$ . As evidenced by the electron micrograph in Figure 5(b), larger pores are visible in the interior of this sample with diameters up to 100  $\mu\text{m}$ . We note that when these experiments were attempted using poly(D,L-lactic acid) (PDLLA) instead of PCL, porous structures of this type were not observed. This may indicate partial miscibility between PDLLA and PEO in the melt state, the possibility of which has already been suggested.<sup>34</sup>

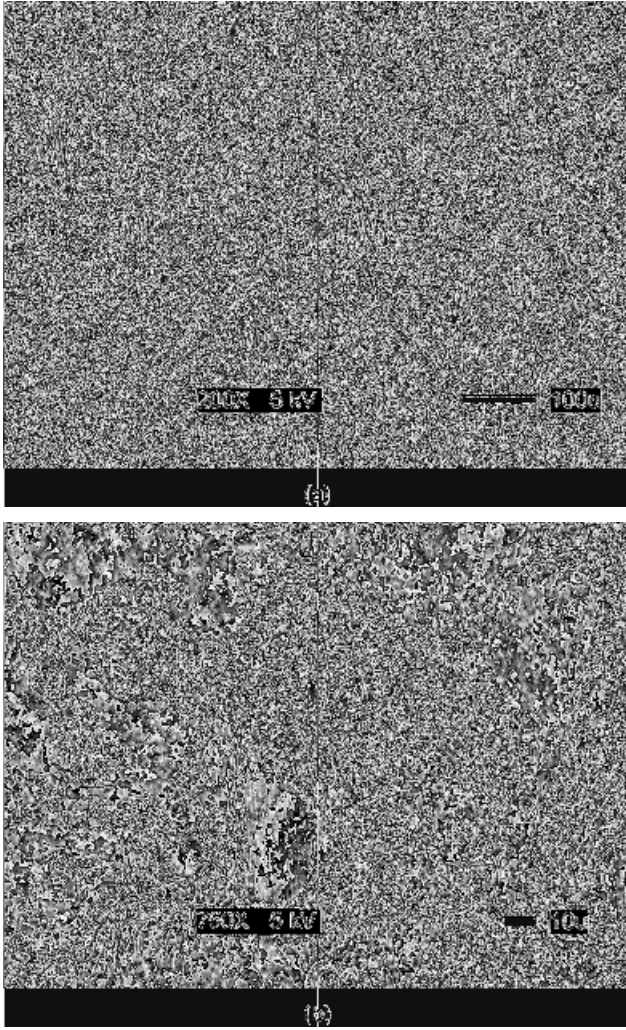


**Figure 5.** (a) Scanning electron micrograph of the surface of the 50% PCL sample after annealing for 20 min at 80°C and subsequent dissolution of PEO. The sample appears to have a continuous network of void space with a characteristic length scale of roughly 50  $\mu\text{m}$ , smaller than that of the 30% PCL sample shown in Figure 4. (b) Interior of the annealed 50% PCL sample that was exposed using a razor blade. The structure was obviously perturbed by cutting but it also appears to be co-continuous with pores ranging from 10 to 100  $\mu\text{m}$ .

It is interesting to note that the anisotropy observed in the unannealed blends is no longer visible in the annealed blends. Because the annealing was done under ambient conditions, the co-continuous blend appears to relax to an isotropic structure, a process that is driven by the interfacial tension. This raises the possibility of generating anisotropic materials with large characteristic length scales through annealing during processing under extensional flow. Given that many biological materials such as collagen and bone are highly anisotropic, development of biomaterials with inherent anisotropies could lead to improvements in tissue engineering applications.

### Compression testing

In Figure 6 are shown plots of stress versus strain for the 30 and 50% PCL annealed samples. The measured moduli at strains below 5% are approximately 1.5 MPa but both data sets display a noticeable curvature with the 50% PCL sample being more pronounced. The low modulus at low strains is attributed to compression of the scaffold microstructure. The 30% PCL sample has more void space than the 50% PCL sample and the scaffold can be compressed more, which is observed in practice. The increase in modulus as a function of strains attributed to a bulk-like response of the material involving irreversible deformations and dislocations of the lattice.<sup>35</sup> Indeed, even the higher moduli observed in these plots are much lower than that observed in nonporous PCL samples, which was measured to be 97 MPa, indicating that the scaffolds are not fully compacted at 20% strain. Because of the relatively low modulus of the matrix material, the low-strain modulus of the PCL scaffolds is lower than that of most reported values of cancellous bone, which has an elastic modulus ranging from approximately 50 to 100 MPa.<sup>36</sup> The current scaffolds are too soft to be used as bone replacement materials but techniques such as fiber reinforcement have shown to lead to biomaterials with improved mechanical properties.<sup>37</sup>

### Biocompatibility studies

In Figure 7 is shown a scanning electron micrograph of a 30% PCL scaffold. Several cells are visible at the top and the right of the image. The osteoblasts have a spread appearance with multiple processes extending outward, indicating that the cells are viable and adhering to these regions of the scaffold. However, even after culturing for 9 days, the cell coverage on the scaffolds is relatively low and inhomogeneous and we propose two possible reasons for this. One is that with a measured water contact angle of  $79.0 \pm 2.6^\circ$ , the bare PCL surface is too hydrophobic to promote cell proliferation and that a presumably inhomogeneous protein coating is responsible for conditioning the polymer surface. The cells would then tend to adhere and proliferate only on conditioned areas. In a study comparing the behavior of marrow stromal cells on polyester surfaces, Calvert et al.<sup>38</sup> demonstrated that cells adhere when cultured on PCL but do not proliferate. Similar control experiments performed in our labs were consistent with this conclusion. Altankov et al.<sup>39</sup> suggested that the ability of cells to reorganize the protein films to which they adhere is important and strongly influenced by the hydrophobicity of the underlying substrate, which may be related to cell proliferation.

Another factor may be the seeding and culturing

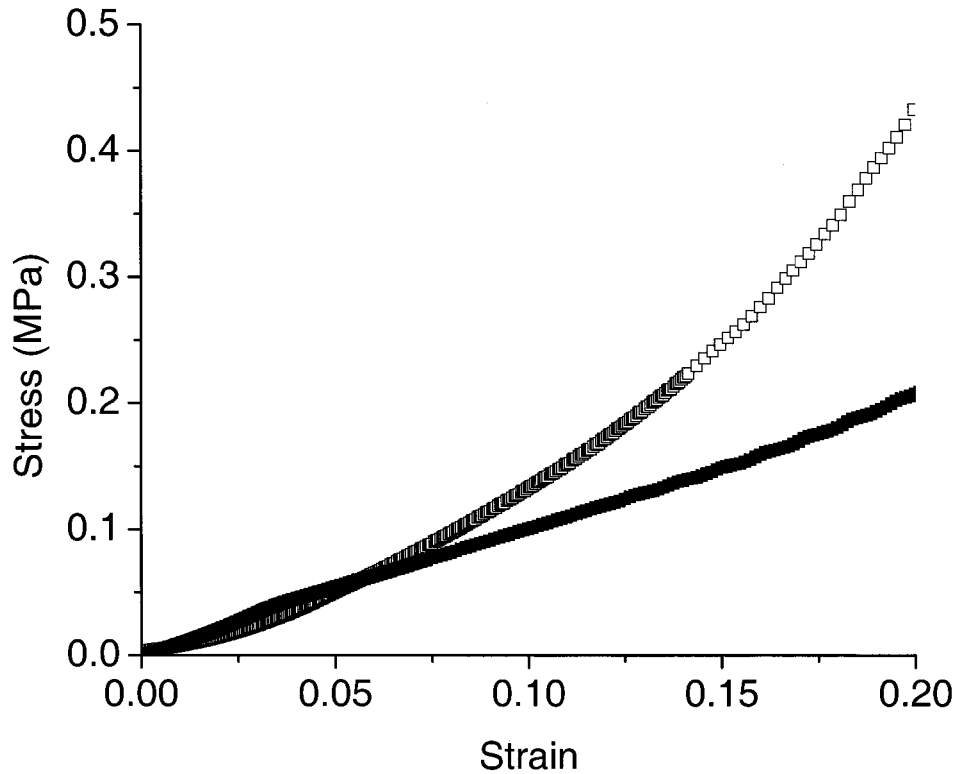


**Figure 6.** Compression testing data for the annealed 30% (filled squares) and 50% (open squares) scaffolds. At low strains, the measured moduli are approximately 1.5 MPa. This is likely associated with compression of the scaffold pores, which is consistent with the faster increase in modulus for the 50% sample.

methods used. Burg et al.<sup>40</sup> performed a thorough investigation of various seeding and culturing methods onto poly(glycolide) scaffolds in which they compared the effects of static, dynamic, and perfusion bioreactor environments. Our experiments were performed using static seeding and static culturing environments. Burg et al. concluded that this led to metabolically

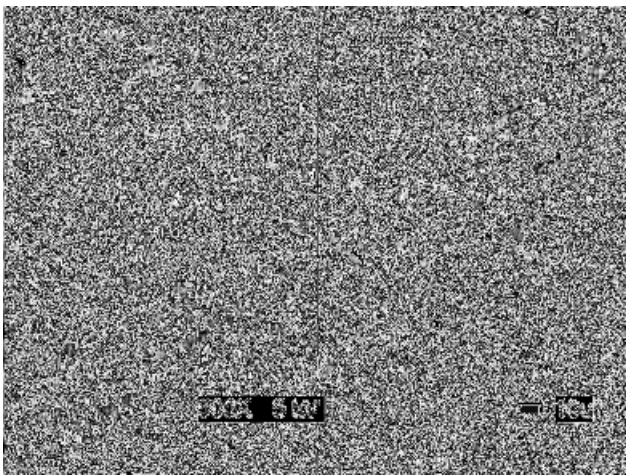


**Figure 7.** Scanning electron micrograph of a cluster of cells on a 30% PCL scaffold. The cells were cultured on the scaffold for 9 days before fixing. The spread, connected morphology suggests that the cells are attached to the substrate and viable.

active clusters of cells and our results are consistent with their findings.

It appears that the large pores of the scaffolds have collapsed by the end of the cell-seeding studies. Because the rate of PCL hydrolysis is quite low,<sup>41</sup> we assume that this was caused by mechanical failure and not chemical decomposition. As was noted, the scaffolds have a spongy feel and it appears they were partially crushed after handling with tweezers and affixing to the bottom of the wells. Future cell studies will require handling the scaffolds with more care. We are also investigating methods for reinforcing the scaffolds by blending PCL with glassy, biocompatible polymers such as poly(D,L-lactic acid).

The cytotoxicity of the extruded material was assessed using a live/dead cell assay 9 days after seeding osteoblasts on the 30% PCL scaffold. In Figure 8 is shown green (a) and red (b) fluorescence microscope images of the same field of view of cells on the surface of the scaffold. Figure 8(a) is the green fluorescence associated with live cells that have taken up calcein-AM. In Figure 8(b) is shown the red fluorescence caused by the uptake of ethidium homodimer-1 by the dead cells in the cell aggregate of Figure 8(a). In this cluster of cells, there are very few dead ones and indeed, only scattered examples visible anywhere on the surface. This suggests that the adherent cells are generally viable.

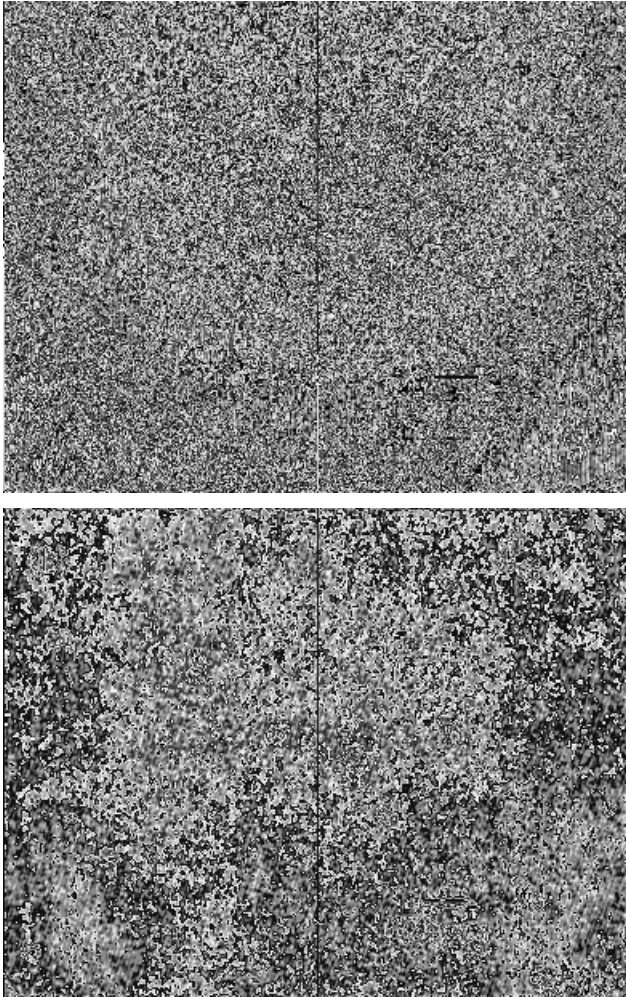


**Figure 8.** (a) Fluorescence micrograph of a cluster of osteoblasts on a 30% PCL scaffold. The fluorescence is from live cells that absorbed calcein. (b) Fluorescence micrograph of the same cluster of cells, some of which are fluorescing red because of ethidium absorption. These cells have weakened membranes and are not viable. However, it appears that most of the cells in this cluster are living.

Although this experiment does not prove the non-toxicity of the co-extruded material, it does suggest these scaffolds are sufficiently nontoxic to sustain cell growth. Further evidence of this comes from observing cells on the bottom of the well containing the seeded scaffolds using phase-contrast light microscopy. A confluent layer of cells was observed (image not shown) indicating that toxic contaminants did not leach out of the scaffolds into the solution.

## CONCLUSIONS

The development of new generalizable techniques for preparing porous polymeric materials for use in tissue engineering continues to be of great interest. We

have demonstrated that co-extrusion may be used to create materials with porous structures having a continuous network of void space. By controlling the blend composition and processing conditions, it is possible to continuously vary the characteristic length scale of the void space up to 100  $\mu\text{m}$ . The blending of biocompatible polymers such as PCL and PEO seems to result in a processed material that retains this biocompatibility, as evidenced by preliminary results from cell studies.

Co-extrusion can also be readily extended to other biodegradable polymers; the only requirement is that the compounded polymers exhibit immiscibility. The "roadmap" for understanding the blending behavior is the rheological characterization of the components. Although the viscoelastic behavior of high polymers and complex extruder flow fields make quantitative predictions of the resulting morphology difficult, a systematic investigation of the processing parameters leads to a good deal of control over the final scaffold material. Finally, with the appropriate equipment, this technique is amenable to both laboratory- and industrial-scale production of polymer scaffolds for tissue engineering.

The authors thank Mr. Anthony Giussipetti for assistance in performing the scanning electron microscopy and compression testing and Dr. Kalman B. Migler for useful discussions.

## References

1. Alexander H, Brunski JB, Cooper SL, Hench LL, Hergenrother RW, Hoffman AS, Kohn J, Langer R, Peppas NA, Ratner BD, Shalaby SW, Visser SA, Yannas IV. Classes of materials used in medicine. In: Ratner BD, Hoffman AS, Schoen FJ, Lemons JE, editors. *Biomaterials science: An introduction to materials in medicine*. San Diego: Academic Press; 1996. p 37–130.
2. Langer RS, Vacanti JP. Tissue engineering: The challenges ahead. *Sci Am* 1999;4:86–89.
3. Hulbert SF, Cooke FW, Klawitter JJ, Leonard RB, Sauer BW, Moyle DD, Skinner HB. Attachment of prostheses to the musculoskeletal system by tissue ingrowth and mechanical interlocking. *J Biomed Mater Res* 1973;7:1–23.
4. Vacanti CA, Langer R, Schloo B, Vacanti JP. Synthetic polymers seeded with chondrocytes provide a template for new cartilage formation. *Plast Reconstr Surg* 1991;88:753–759.
5. Yannas IV, Lee E, Orgill DP, Skrabut EM, Murphy GF. Synthesis and characterization of a model extracellular matrix that induces partial regeneration of adult mammalian skin. *Proc Natl Acad Sci USA* 1989;86:933–937.
6. Moyer B, Lahey PJ, Weinberg EH, Harris WH. Effects on intact femora of dogs of application of metal plates. *J Bone Joint Surg Am* 1978;60:940–947.
7. Cook AD, Hrkach JS, Gao NN, Johnson IM, Pajvani UB, Cannizzaro SM, Langer R. Characterization and development of RGD-peptide-modified poly(lactic acid-co-lysine) as an interactive, resorbable biomaterial. *J Biomed Mater Res* 1997;35: 513–523.

8. Vert M, Li SM. Bioresorbability and biocompatibility of aliphatic polyesters. *J Biomed Mater Res* 1992;3:432–446.
9. Ishaug SL, Yaszemski MJ, Bizios R, Mikos AG. Osteoblast function on synthetic biodegradable polymers. *J Biomed Mater Res* 1994;28:1445–1453.
10. Ishaug-Riley SL, Crane-Kruger GM, Yaszemski MJ, Mikos AG. Three-dimensional culture of rat calvarial osteoblasts in porous biodegradable polymers. *Biomaterials* 1998;19:1405–1412.
11. Widmer MS, Gupta PK, Lu L, Meszlenyi RK, Evans GRD, Brandt K, Savel T, Gurlek A, Patrick CW, Mikos AG. Manufacture of porous biodegradable polymer conduits by an extrusion process for guided tissue regeneration. *Biomaterials* 1998;19:1945–1955.
12. Schugens Ch, Maquet V, Grandfils C, Jerome R, Teyssie Ph. Biodegradable and macroporous polylactide implants for cell transplantation. I. Preparation of macroporous polylactide supports by solid–liquid phase separation. 1996;37:1027–1038.
13. Whang K, Thomas CH, Healy KE, Nuber G. A novel method to fabricate bioabsorbable scaffolds. *Polymer* 1995;36:837–842.
14. Aubert JH, Clough RL. Low-density, microcellular polystyrene foams. *Polymer* 1985;26:2047–2055.
15. Schugens C, Maquet V, Grandfils C, Jerome R, Teyssie P. Polylactide macroporous biodegradable implants for cell transplantation. II. Preparation of polylactide foams by liquid–liquid phase separation. *J Biomed Mater Res* 1996;30:449–461.
16. Schugens C, Grandfils C, Jerome R, Teyssie P, Delree P, Martin D, Malgrange B, Moonen G. Preparation of a macroporous biodegradable polylactide implant for neuronal transplantation. *J Biomed Mater Res* 1995;29:1349–1362.
17. Park A, Wu B, Griffith LG. Integration of surface modification and 3D fabrication techniques to prepared patterned poly(L-lactide) substrates allowing regionally selective cell adhesion. *J Biomater Sci Polym Ed* 1998;9:89–110.
18. Hutmacher DW, Schantz T, Zein I, Ng KW, Teoh SH, Tan KC. Mechanical properties and cell cultural response of polycaprolactone scaffolds designed and fabricated via fused deposition modeling. *J Biomed Mater Res* 2001;55:203–216.
19. Agassant J-F, Avenas P, Sergent J-P, Carreau PJ. *Polymer processing*. Munich: Hanser Publishers; 1991. 475 p.
20. Tadmor Z, Gogos CG. *Principles of polymer processing*. New York: John Wiley & Sons; 1979. 735 p.
21. Cima LG. Polymer substrates for controlled biological interactions. *J Cell Biochem* 1994;56:155–161.
22. Utracki LA. On the viscosity-concentration dependence of immiscible polymer blends. *J Rheol* 1991;35:1615–1637.
23. Paul DR, Barlow JW. Polymer blends (or alloys). *J Macromol Sci Rev Macromol Chem* 1980;C18:109–168.
24. Jordhamo GM, Manson JA, Sperling LH. Phase continuity and inversion in polymer blends and simultaneous networks. *Polym Eng Sci* 1986;26:517–524.
25. Mimura K, Ito H, Fujioka H. Improvement of thermal and mechanical properties by control of morphologies in PES-modified epoxy resins. *Polymer* 2000;41:4451–4459.
26. George SC, Ninan KN, Groeninckx G, Thomas S. Styrene-butadiene rubber/natural rubber blends: Morphology, transport behavior, and dynamical mechanical and mechanical properties. *J Appl Polym Sci* 2000;78:1280–1303.
27. Lee JK, Han CD. Evolution of a dispersed morphology from a co-continuous morphology in immiscible polymer blends. *Polymer* 1999;40:2521–2536.
28. Attawia MA, Uhrich KE, Botchwey E, Langer R, Laurencin CT. *In vitro* bone biocompatibility of poly(anhydride-co-imides) containing pyromellitylimidoalanine. *J Orthop Res* 1996;14:445–454.
29. Gear ARL. Rapid platelet morphological changes visualized by scanning electron microscopy: Kinetics derived from a quenched-flow approach. *Br J Haematol* 1984;56:387–398.
30. Bray DF, Bagu J, Koegler P. Comparison of hexamethyldisilazane (HMDS), Peldri II, and critical-point drying methods for scanning electron microscopy of biological specimens. *Microsc Res Tech* 1993;26:489–495.
31. Macosko CW. *Rheology: Principles, measurements, and applications*. New York: VCH Publishers; 1994. 550 p.
32. Willemse RC, Posthuma de Boer A, van Dam J, Gotsis AD. Co-continuous morphologies in polymer blends: The influence of the interfacial tension. *Polymer* 1999;40:827–834.
33. Wise GM, Denn MM, Bell AT, Mays JW, Hong K, Iatrou H. Surface mobility and slip of polybutadiene melts in shear flow. *J Rheol* 2000;44:549–567.
34. Nijenhuis AJ, Colstee E, Grijpma DW, Pennings AJ. High molecular weight poly(L-lactide) and poly(ethylene oxide) blends: Thermal characterization and physical properties. *Polymer* 1996;37:5849–5857.
35. Ward IM. *Mechanical properties of solid polymers*. New York: John Wiley & Sons; 1983. 475 p.
36. Gibson LJ. The mechanical behaviour of cancellous bone. *J Biomech* 1985;18:317–328.
37. Haers PE, Sailer HF. Biodegradable self-reinforced poly-L/DL-lactide plates and screws in bimaxillary orthognathic surgery: Short term skeletal stability and material related failures. *J Craniomaxillofac Surg* 1998;26:363–372.
38. Calvert JW, Marra KG, Cook L, Kumta PN, DiMilla PA, Weiss LE. Characterization of osteoblast-like behavior of cultured bone marrow stromal cells on various polymer surfaces. *J Biomed Mater Res* 2000;52:279–284.
39. Altankov G, Grinnell F, Groth T. Studies on the biocompatibility of materials: Fibroblast reorganization of substratum-bound fibronectin on surfaces varying in wettability. *J Biomed Mater Res* 1996;30:385–391.
40. Burg KJL, Holder WD Jr, Culberson CR, Beiler RJ, Greene KG, Loeb sack AB, Roland WD, Eiselt P, Mooney DJ, Halberstadt CR. Comparative study of seeding methods for three-dimensional polymeric scaffolds. *J Biomed Mater Res* 2000;51:642–649.
41. Pitt CG, Chasalow FI, Hibionada YM, Klimas DM, Schindler A. Aliphatic polyesters. I. The degradation of poly( $\epsilon$ -caprolactone) *in vivo*. *J Appl Polym Sci* 1981;28:3779–3787.